Ballistic protection against armour piercing projectiles using titanium base armour

Diederen, A.M.¹, Broos, J.P.F.¹, Trigt, S.N. van¹, Peijen, M.C.P.²

¹ TNO Prins Maurits Laboratory, P.O. Box 45, NL-2280 AA Rijswijk, The Netherlands ² Royal Netherlands Army, Directorate of Materiel, P.O. Box 90822, NL-2509 LV The Hague

Abstract

This paper presents the experimentally established ballistic resistance of armour configurations with titanium base armour against 12.7 mm AP, 14.5 mm AP and 25 mm APDS projectiles. The target configurations consist of a very hard outer layer, a Ti-6Al-4V base armour and sometimes a polyethylene composite spall-liner. The ballistic limit velocity distribution according to the Kneubuehl method is established for 12.7 mm AP / 14.5 mm AP ammunition (0° or 60° NATO impact angle). The areal density of the tested armour configurations can be compared with other modern (aluminium base) armour configurations using a single graph per stopping probability (e.g. 99%). The titanium-based targets are overmatched and perforated by 25 mm APDS projectiles. For this threat and for normal impact, the spall cone characteristics and the residual projectile penetration are established using metallic witness-packs. The hole-size distribution gives the cone angle and spall density distribution, the difference in hole-size distribution from the first (front) to the last witness plate indicates the penetration capacity distribution of the spall cloud. Different thicknesses of spall-liner backing the titanium armour are used to assess their effectiveness.

1. Introduction

In 1999, we presented a number of test results with armour configurations mainly based on aluminium armour representing the hull of a light to medium armoured vehicle [1]. Besides aluminium, also titanium base armour has been used because of its weight benefits. Application of a thin spall-liner showed a significant increase of the threshold velocity when combined with an armour configuration that is almost balanced against the concerning threat. This paper discusses the continuation of these tests with titanium base armour and spall-liners, both with Russian 14.5 mm AP-I B32 (steel core) projectiles and 25 mm APDS projectiles for assessment of liner application in an overmatch-situation (target only stops 14.5 mm AP). In a number of cases, alternatively Russian 14.5 mm AP-I BS41 (tungsten carbide core) and Dutch 12.7 mm API 2000 (tungsten carbide core) have been used.

The armour configurations will be compared to one another based on their V99 (99% stopping probability if possible for two reasons. First this is much closer to real protection requirements than for instance the V50 (50% stopping probability). Second the sequence of performance of armour configurations can be different when based on the V99 instead of the V50.

2. Armour configurations

Table 1 gives an overview of the applied armour configurations (range targets or in short "targets"), which are depicted in Annex A. The threat used was the Russian 14.5 mm AP-I B32 projectile and/or the treat mentioned in the column "Remarks".

Table 1

Range	Impact	outer layer	airgap	Base	Liner	Results	Remarks
target	angle			armour			
6	$0_{\mathbf{o}}$	ARMOX-600S	yes	Ti-6Al-4V	-	V99	
7	$0_{\mathbf{o}}$	ARMOX-600S	yes	Ti-6Al-4V	Dyneema	V99	
8	60°	SPS-43	yes	Ti-6Al-4V	-	V99	
14	0_{o}	ARMOX-600S	yes	Ti-6Al-4V	Dyneema	V99	also 25 APDS overmatch
15	$0_{\mathbf{o}}$	LIBA/composite	no	Ti-6Al-4V	Dyneema	-	also 14.5 BS41
16	60°	ARMOX-600S	yes	Ti-6Al-4V	Dyneema	-	also 14.5 BS41 at 45°
17	60°	MARS-300 perf	yes	Ti-6Al-4V	Dyneema	=	also 14.5 BS41 at 45
18	0_{o}	LIBA/composite	no	Ti-6Al-4V	-	V99	12.7 API 2000

Target 6 consists of a spaced array of HH (high hardness) steel and titanium of equal plate thickness, target 7 is equal to target 6 but with a thin Dyneema spall-liner attached (see Annex A). Target 8 uses the same titanium plate as targets 6 and 7 but is combined with a thin HH steel plate and impacted at 60° NATO.

In order to reduce the areal density of target 7, target 14 uses a thicker titanium and a thinner HH steel plate. Target 14 is also used with a number of thicker Dyneema spall-liners for overmatch-situations (25 mm APDS).

Target 15 uses the same titanium plate as target 14 and is combined with an outer layer of ceramic pellets to combine the successful targets of our previous work [1] and expand our experiments to 14.5 mm BS41 tungsten carbide core projectiles. Unfortunately, as will be discussed in §5.1, target 15 is too weak to stop 14.5 mm BS41 and too strong to let 14.5 mm B32 (steel core) perforate, so a part of the titanium plate thickness has been removed to make target 18 with lower areal density. Target 18 is still too strong to let 14.5 mm B32 perforate, but its V99 could be established against 12.7 mm API 2000 (tungsten carbide core) projectiles.

Targets 16 and 17 were intended to assess their performance against 14.5 mm BS41 but could not be perforated at 60° NATO, so no threshold velocity has been established.

The lateral target dimensions for the 12.7 / 14.5 mm AP experiments are $500 \times 500 \text{ mm}$, except for the thin Dyneema spall-liners which have lateral dimensions of $460 \times 460 \text{ mm}$. The lateral target dimensions for the 25 mm APDS experiments, conducted with target 14, are $300 \text{ mm} \times 300 \text{ mm}$. The (apparent) density ' ρ ' (see text below) of the armour plates has been determined by measuring the dimensions and weighing the plates.

Three types of HH steel have been used:

- ARMOX-600S, manufactured by Swedish Steel, $\rho = 7.84 \text{ g/cm}^3$, Brinell hardness around 600 HB.
- SPS-43, manufactured by Special Materials, St. Petersburg, Russia, $\rho = 7.63$ g/cm³, hardness around 500 HB.
- MARS-300 perforated, manufactured by Creusot-Loire of France, $\rho = 4.09$ g/cm³, hardness around 600 HB.

For titanium, the customary alloy Ti-6Al-4V has been used. The titanium armour plates for targets 6, 7 and 8 have been cut from a large plate of 'Tikrutan LT31' with a Brinell hardness of around 300 HB, manufactured by Deutsche Titan of Germany. The measured density is 4.45 g/cm³. The titanium armour plates for the other targets have a similar density and hardness and were manufactured by US companies.

LIBA (Light Improved Ballistic Armour) consists of very hard ceramic pellets in a matrix of a polyurethane rubber / resin mixture. It is an Israeli invention [2] and is marketed for Europe by Ten Cate Advanced Composites of The Netherlands.

The LIBA together with the composite backing was clamped directly to the titanium base armour using screw clamps and quick-acting clamps. The measured density of the combination of LIBA and composite backing is 2.48 g/cm³.

The Dyneema polyethylene fibre spall-liner, type UDX-75 HB2, is manufactured by DSM High Performance Fibers of The Netherlands. The measured density varies from 0.92 to 0.98 g/cm³.

The Dyneema is mounted on the titanium base armour of target 7 by means of 5 bolts (4 at the corners and one at the centre). All other targets (including for 25 mm APDS impact) only used the 4 corner bolts. The Dyneema backings for the 25 mm APDS tests were also adhesively bonded to the titanium base armour.

3. Test set-up

3.1 Experiments with 12.7 / 14.5 mm AP

The targets are mounted on an adjustable frame (0° to almost 90° NATO) using screw clamps and quick-acting clamps. The armour plates are spaced from one another using square tubular sections at the perimeter of the armour plates. The weapon is placed at a fixed position; the target is shifted before each shot so an undamaged part can be impacted. The distance between weapon and target is 28.7 meters for the 14.5 mm AP projectiles (around 9 meters for 12.7 mm AP). The impact velocity of the projectile is registered just in front of the target by means of 2 light screens (see figure 1). For a number of experiments high-speed photography recordings have been made using an Imacon 468 camera (see figure 1).

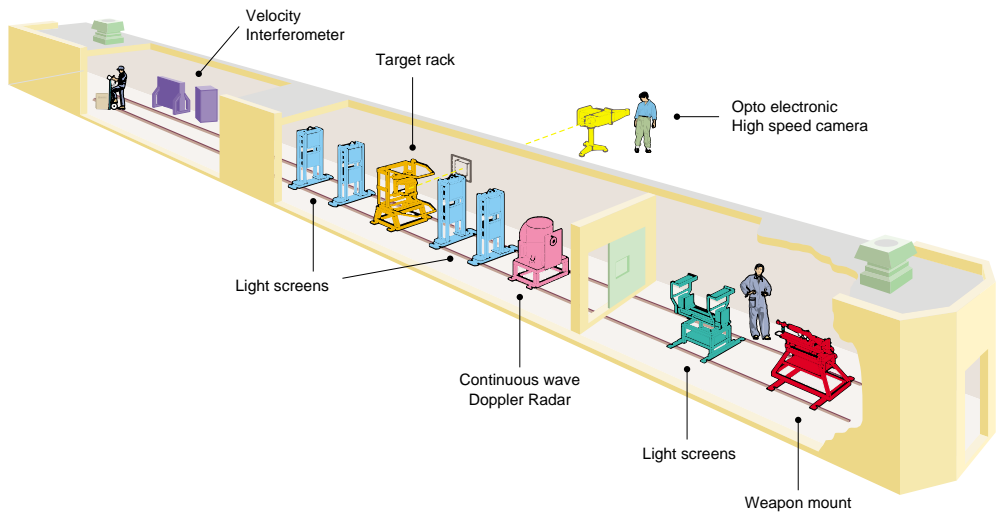


Figure 1: Small-calibre test range at TNO Prins Maurits Laboratory

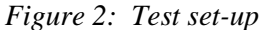
In order to determine the threshold velocity (V50, V90, and so on), a number of shots have to perforate the target and a number of shots have to be stopped by the target. For this reason for a large number of shots the amount of gunpowder in the cartridge has to be diminished to establish a lower impact velocity (corresponding with a larger shooting distance). For a limited number of shots the amount of gunpowder has been slightly increased to establish a sufficient number of perforations.

3.2 Experiments with 25 mm APDS

The projectiles were 25 mm APDS, type nr. 121 from Oerlikon. All tests were conducted at full velocity (muzzle velocity around 1335 m/s) with normal impact at the centre of the targets.

The right part of figure 2 shows the X-ray cassettes which establish the orthogonal yaw of the projectile (the foil to the right triggers the concerning X-rays). The left part of figure 2 shows the target mounted on a frame (including second triggerfoil for impact velocity measurement). Figure 3 gives a close-up of the target (showing the ARMOX-600S plate spaced from the titanium base armour and Dyneema liner of target 14), 500 mm behind the target the front of the metallic witness-pack can be seen (see also figure 6).





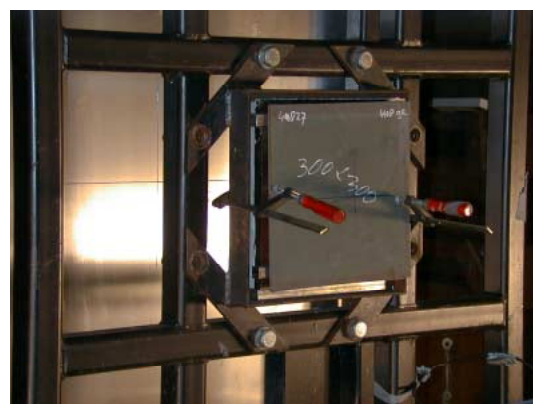


Figure 3: Test set-up (front view of target)

Figure 5 shows (at the right) the witness-pack behind the target and (at the left) the thick steel witness-plate (spaced 500 mm from the witness-pack) to measure the penetration depth of the residual projectile or projectile parts.



Figure 5: Witness-pack (right) and thick witness-plate (left)

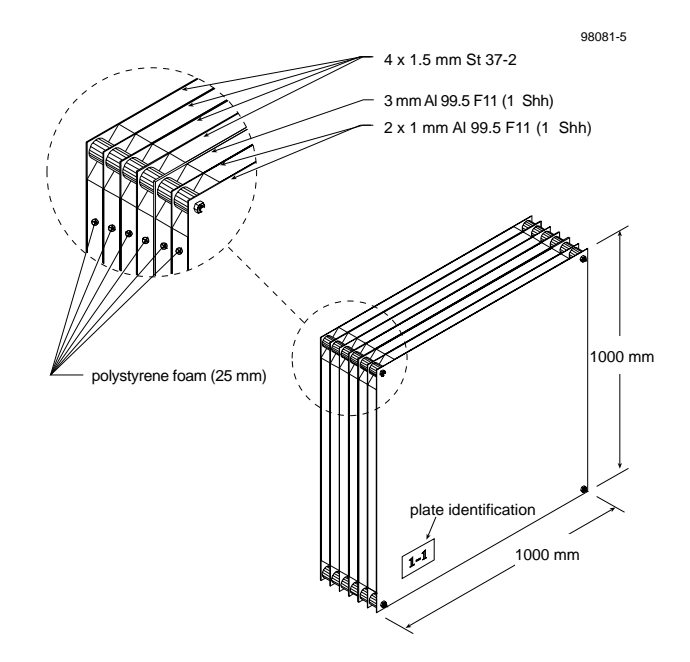


Figure 6: Witness-pack type M1 according to STANAG 4190

4. Kneubuehl method (12.7 / 14.5 mm AP experiments)

The threshold velocities (V50, V90, and so on) are determined according to the Kneubuehl method [3]. This requires a minimum number of 12 shots. The difference between this method and the V50-determination according to STANAG 2920 is that the Kneubuehl method takes the standard deviation into account. By so doing, the threshold velocity is determined as a function of impact velocity instead of determining only one specific threshold velocity (V50: 50% stopping probability). By using the Kneubuehl method, not only the V50 is established but also the sensitivity for decreasing or increasing the impact velocity (shooting distance). This is important, because an armour which is in favour of another armour based only on the V50 (see solid line opposed to dashed line in example of figure 6) can perform worse than the other armour at a lower impact velocity (in this example a lower V90 than the other armour).

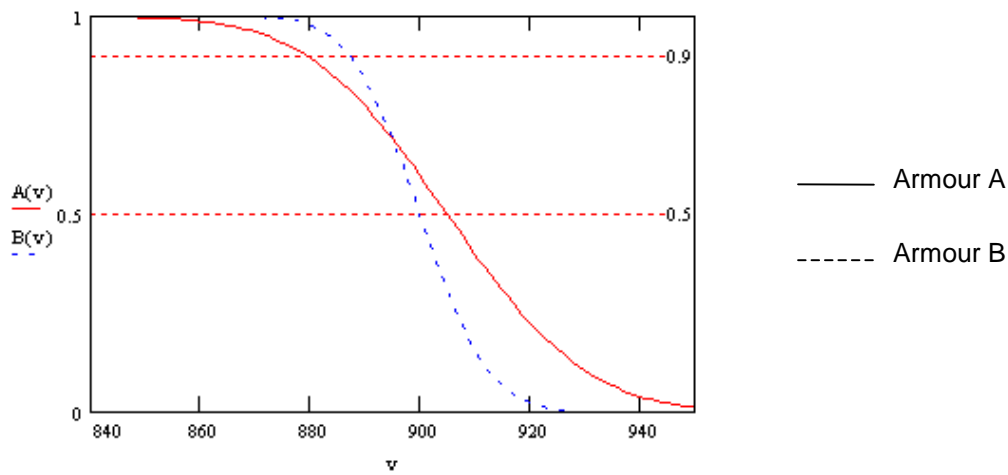


Figure 6: Example of threshold velocities as a function of impact velocity (vertical axis: stopping probability; horizontal axis: impact velocity).

Given the V50 and the standard deviation ' σ ' of an armour configuration, the stopping probability 'P' for any impact velocity 'V_t' can be estimated using the formula [3]:

$$P(V_{t}) = 1 - \frac{1}{\sqrt{2\pi \cdot \sigma}} \int_{-\infty}^{V_{t}} e^{-\frac{1}{2}(\frac{V - V \cdot 50}{\sigma})^{2}} dV$$

5. Results

5.1 Results for 12.7 / 14.5 mm AP

For targets 6, 7, 8, 14 and 18 (see tables 1 and 2) 12 to 20 shots have been performed. The impact velocities have been chosen in such a way that both stops and perforations have been realised so that the threshold velocities (see table 2) could be established. The V50 corresponds with an estimated stopping probability of 50%, the V90 corresponds with an estimated stopping probability of 90%, and so on. The areal densities (kg/m²) are given relative to RHA required to stop the threat (14.5 mm AP-I B32).

Note that target 18 has been tested against 12.7 mm API 2000 (tungsten carbide core) which is a heavier threat than 14.5 mm AP-I B32 (steel core).

7	¬	1_	1 _	1
1	a	D	ıe	_

Tubic 2						
Range	Impact	V50 [m/sec]	V90 [m/sec]	V99 [m/sec]	Standard	Areal density
target	angle				deviation	relative to RHA
					[m/sec]	(RHA=100%)
6	$0_{\mathbf{o}}$	905	889	875	12.8	50.4
7	$0_{\mathbf{o}}$	994	980	969	10.7	52.0
8	60°	880	856	836	18.7	49.8
14	$0_{\mathbf{o}}$	909	884	864	19.5	47.3
15	$0_{\mathbf{o}}$					56.1
16	60°					(62.7)
17	60°					(54.0)
18	$0_{\mathbf{o}}$	867	830	799	29.0	(47.9)

For targets 15, 16 and 17 no threshold velocity distribution (a.o. V99, \geq 12 valid shots) or V50 threshold velocity (\geq 6 valid shots) could be established.

Target 15 was originally intended for V99 establishment against 14.5 mm AP-I BS41, but proofed too weak to even stop this tungsten carbide core projectile at a reduced velocity of 780 m/s. On the other hand, the 14.5 mm AP-I B32 steel core projectile couldn't even perforate target 15 at full velocity (up to 1,007 m/s). Here, the titanium surface at impact side is only scratched. Obviously, the applied Al₂O₃-based ceramic pellets of the LIBA are hard enough to shatter the steel core projectile, whereas the tungsten carbide core projectile is harder than the LIBA-pellets and stays intact enough to perforate the titanium base armour. Figure 7 shows the impact side of the titanium base armour with 1 stop (14.5 mm AP steel core) and 3 perforations (14.5 mm AP tungsten carbide core).

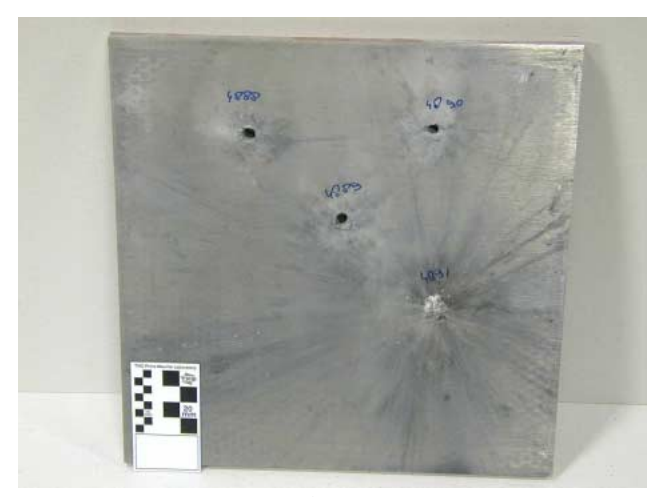


Figure 7: Titanium base armour of target 15

In order to obtain a V99 establishment, the titanium plates of the targets according to armour configuration 15 were machined to reduce their thickness by some 25%. The adapted target still proofed too strong for 14.5 mm AP steel core, but the 12.7 mm API 2000 with tungsten carbide core can penetrate at full velocity. By omitting the thin Dyneema liner, a V99 could be established and the range target name has been designated target 18.

Both target 16 and target 17 proofed too strong against 14.5 mm AP-I BS41 (tungsten carbide core) projectiles. The targets (60° NATO) could not be perforated at full velocity, at 45° NATO perforation could be achieved at around 900 m/s for both target 16 and 17.

Figure 8 is a graphical representation of the results (V50, V90 and V99) for normal impact, including previous results with aluminium base armour configurations [1] as a reference. It shows the influence of the standard deviation (or spread in the results) on the relative performance of the armour configurations.

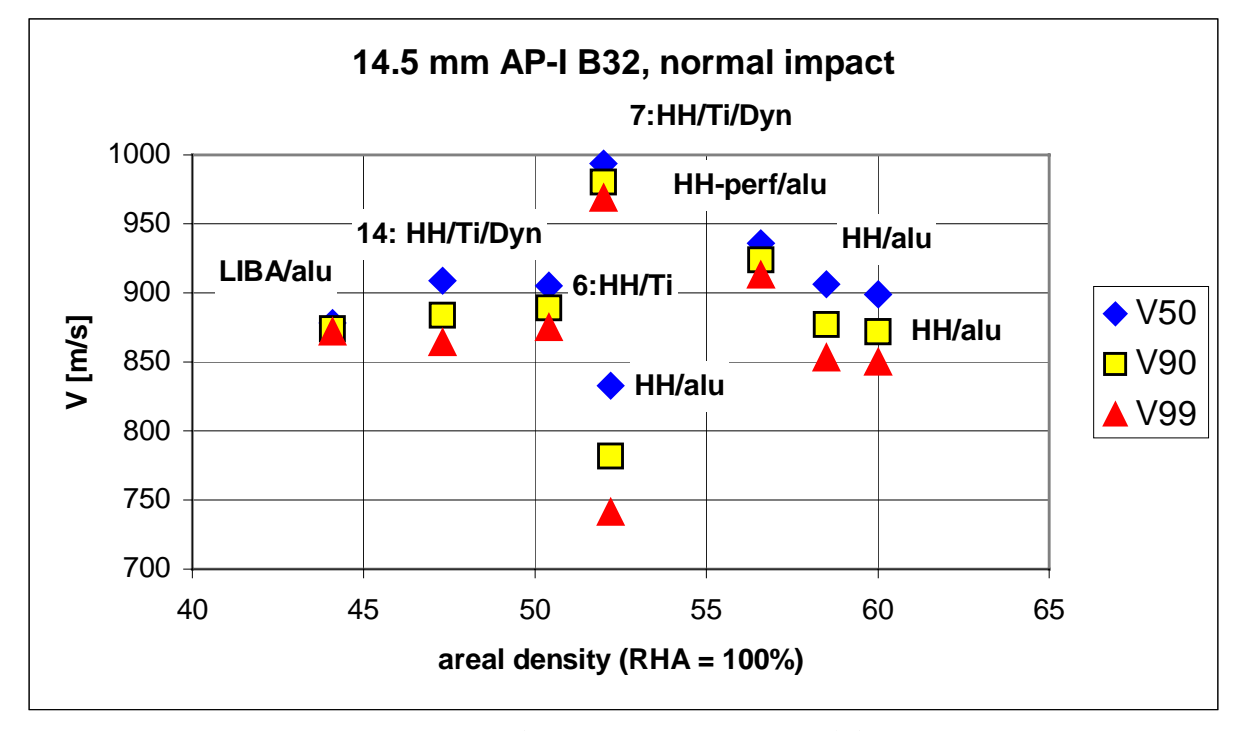


Figure 8: V50, V90 and V99 as a function of areal density

Figure 9 gives the required areal density (relative to RHA) for the armour configurations impacted at 0° NATO to realise an estimated stopping probability of 99%. For the targets impacted at 60° NATO see [1]. At the right of figure 9 the shooting distance corresponding with the impact velocity along the vertical axis is given, based on MIL-Std-662E, Issue 94-04.

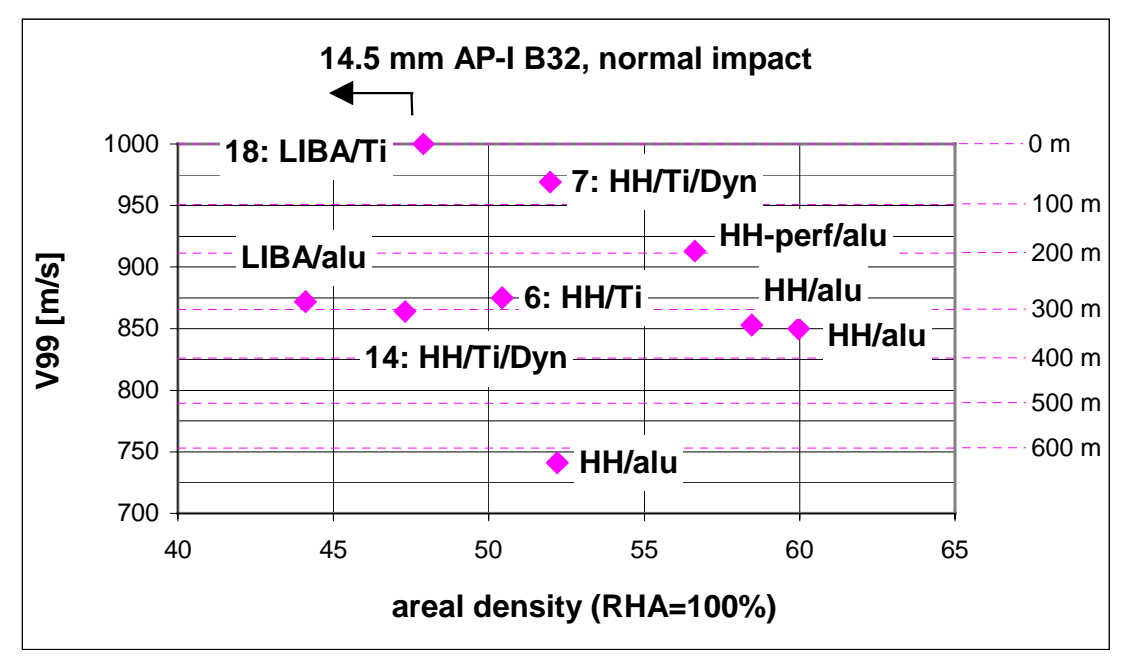


Figure 9: Required areal densities for an estimated stopping probability of 99%, 0° NATO impact

Target 18, although tested against 12.7 mm API 2000, is incorporated in figure 9 to show that this type of armour configuration (LIBA / titanium) will need an areal density much less than the concerning point in the graph of figure 9 to stop 14.5 mm AP-I B32.

Target 14 clearly shows the benefit of optimising the thickness of the layers of a specific armour configuration: target 14 uses thicker titanium and thinner HH-steel compared with target 7. The possibility to further reduce the areal density of this type of armour configuration is very likely, but this would call for simulations to reduce the number of experiments and the use of target material.

5.2 Results for 25 mm APDS

Figures 10 to 13 show the hole patterns in the first three witnessplates of a reference target (no liner, figure 10) and the targets with a 10, 15 and 20 mm thick Dyneema liner respectively (figures 11, 12 and 13 respectively). The emission angle of the spall cone is reduced with increasing liner thickness as one would expect. Application of a 20 mm thick Dyneema liner (bolted and adhesively bonded) behind the titanium base armour of target 14 and perforated by a 25 mm APDS projectile (overmatch) results in an emission angle reduction from 35°-40° to 15°-20° for the first witnessplate and to 10°-15° for the third witnessplate. This is better visualised in figures 14 and 15 representing the first witnessplates of the reference target of figure 10 and the target with 20 mm Dyneema of figure 13.

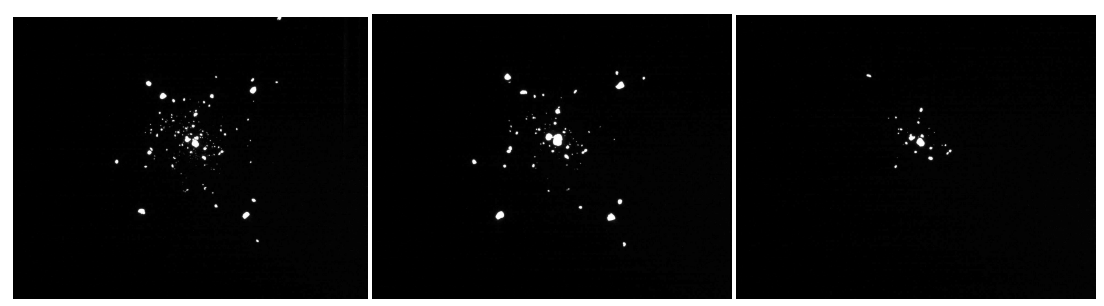


Figure 10: First (left), second (middle) and third (right) witnessplate of target 14 without a liner

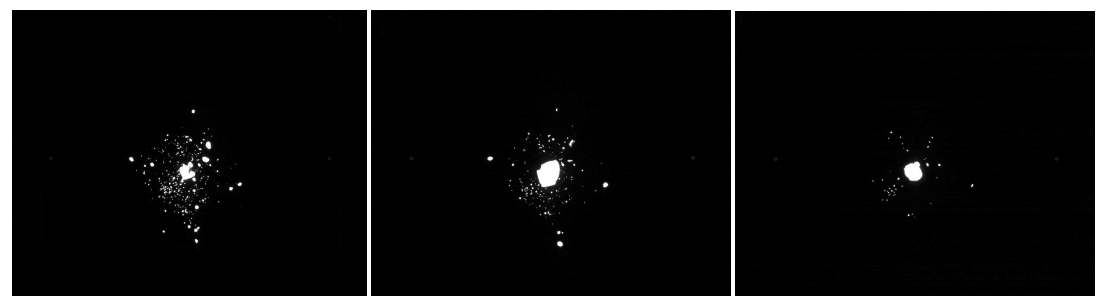


Figure 11: First (left), second (middle) and third (right) witnessplate of target 14 with a 10 mm Dyneema liner



Figure 12: First (left), second (middle) and third (right) witnessplate of target 14 with a 15 mm Dyneema liner

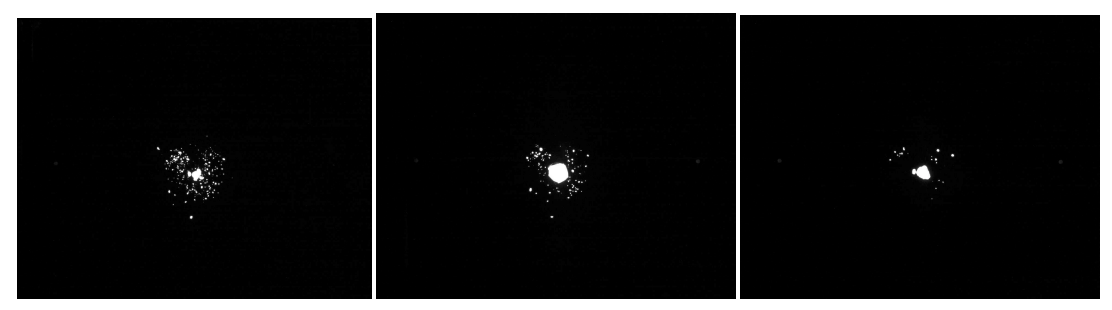


Figure 13: First (left), second (middle) and third (right) witnessplate of target 14 with a 20 mm Dyneema liner

Each marker in figure 14 and 15 is a perforation hole. The inner circle represents an emission angle of 5° and the outer circle represents an emission angle of 45°, all circles in-between are spaced 5° from each other. The Dyneema liner creates a kind of focusing effect, resulting in more fragments perforating the first witnessplate at the inner emission angles and less fragments hitting the larger emission angles as compared to the reference target without a

liner. Figure 16 shows a rear-view and a side-view on the target with the 20 mm Dyneema liner.

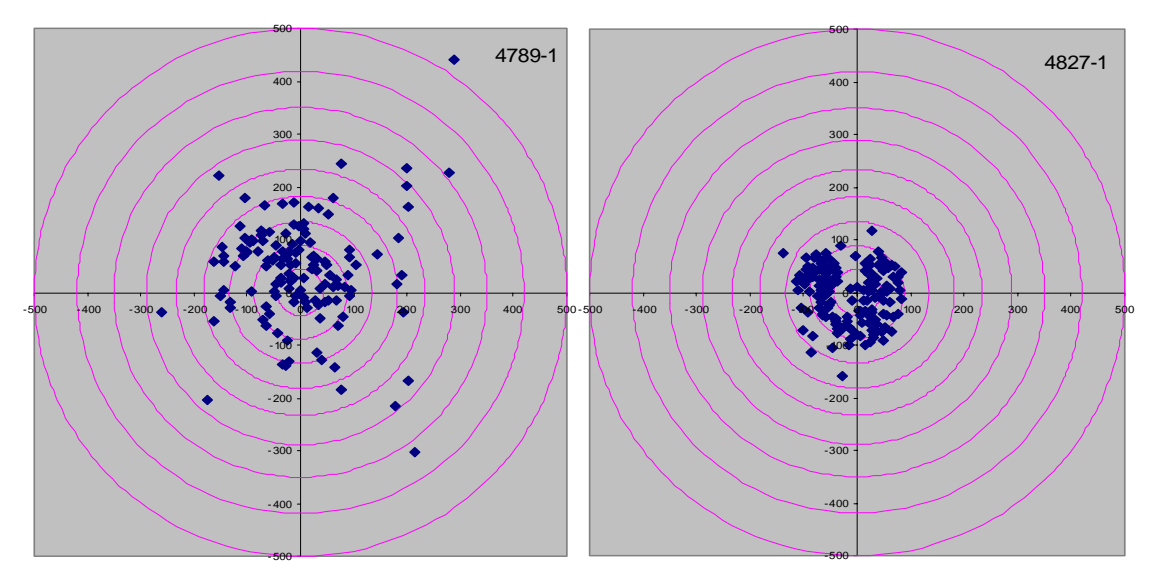


Figure 14: First witnessplate of target 14 without a liner

Figure 15: First witnessplate of target 14 with a 20 mm Dyneema liner





Figure 16: 20 mm Dyneema liner after perforation

In open literature it is indicated that a titanium armour plate results in "more spall" than a steel armour plate of comparable strength and under similar conditions (type of projectile, impact velocity and impact angle). We compared the two reference tests with titanium base armour (one of them is pictured in figure 10) to three tests with steel armour. Both the tests with titanium and steel result in the same shallow penetration craters in the thick witnessplate behind the witnesspack, indicating that the ballistic resistance is comparable. Figures 17 and

18 show representative results of the reference tests with titanium (figure 17 which is equal to figure 10) and of the tests with steel (figure 18).

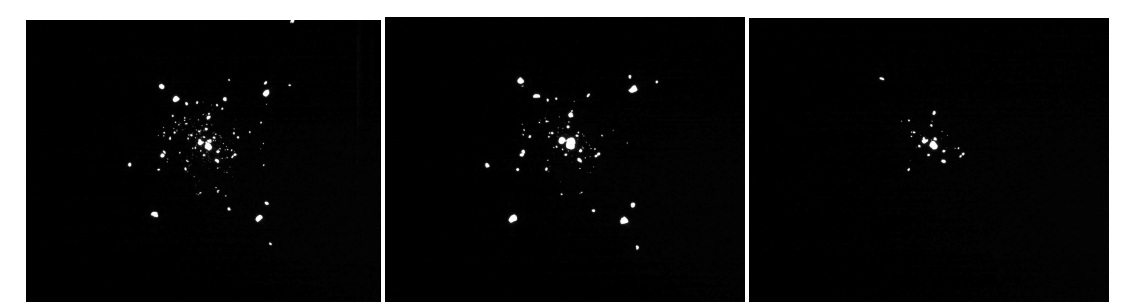


Figure 17: First (left), second (middle) and third (right) witnessplate of target 14 without a liner (equal to figure 10)



Figure 18: First (left), second (middle) and third (right) witnessplate of a steel armour target

The titanium targets show more holes in the first witnessplate (for emission angles of 10° and more) but less holes in the third witness plate as compared to the steel targets. This can be explained as follows. The loss of mass of the base armour shows that the titanium base armour produces 22% less fragments by weight (on average) than the steel armour. However, the compounded volume of all fragments with the titanium base armour is almost 40% larger than with the steel armour because of the difference in density (7.85 g/cm³ for steel and 4.45 g/cm³ for titanium). This explains the larger numbers of holes (for emission angles of 10° and more) in the first witnessplate with titanium. Because the titanium fragments have a lower density than the steel fragments and because the total mass of titanium fragments is lower than with steel, the rear witnessplates are penetrated less when the titanium base armour is applied.

6. Conclusions

For normal impact and for 99% stopping probability (V99 threshold velocity), the areal densities range from around 60% (HH steel plus aluminium) to less than 45% (LIBA plus aluminium) of the areal density of RHA required to stop the threat (14.5 mm AP-I B32 steel core). The weightsaving in titanium base armour configurations by simply changing the thickness of the layers together with the results for LIBA/titanium armour (V99 of around 800 m/s against 12.7 mm API 2000 tungsten carbide core) indicate that areal densities of around 40% are feasible based on titanium base armour.

The indication encountered in open literature that titanium produces more spall than steel armour under similar conditions needs some adjustment. With the concerning overmatch

situation (25 mm APDS against an armour capable of stopping 14.5 mm AP steel core) the compounded volume of all fragments is larger with titanium armour than with steel armour, resulting in a larger number of holes in the first witnessplate. But because the titanium fragments have a lower density than the steel fragments and because the total mass of titanium fragments is lower than with steel armour, the penetration capacity into the rear witness plates is less with titanium armour.

Application of Dyneema liners behind the titanium base armour results in a focussing effect of the fragments for the chosen overmatch situation: the inner emission angles receive more and the outer emission angles receive less fragments than with titanium armour without a liner. Application of a 20 mm thick Dyneema liner (bolted and adhesively bonded) behind the titanium base armour results in an emission angle reduction from $35^{\circ}-40^{\circ}$ to $15^{\circ}-20^{\circ}$ for the first witnessplate and to $10^{\circ}-15^{\circ}$ for the third witnessplate.

References

- [1] Diederen, A.M., Broos, J.P.F., Peijen, M.C.P., *Modern armour configurations against 14.5 mm AP*, Lightweight Armour Systems Symposium, 10-12 November 1999, Royal Military College of Science, Shrivenham, United Kingdom.
- [2] Cohen, M., Israeli, A., *Composite armor panel and manufacturing method thereof*, European Patent Specification EP 0 843 149 B1, date of publication and mention of the grant of the patent: 26.08.1998.
- [3] Kneubuehl, B.P., *Improved test procedure for body armour. Statistical base and evaluation program*, Personal Armour Systems Symposium 1996, pp. 287-294, 3-6 September 1996, Colchester, United Kingdom.

Annex A: Armour configurations

